BIOCHEMISTRY
including biophysical chemistry & molecular biology
Article

Biochemistry **2010,** *49,* 3715–3722 3715
DOI: 10.1021/bi100130f

Biochemical and Pharmacological Analyses of HIV-1 Integrase Flexible Loop Mutants Resistant to Raltegravir[†]

Mathieu Métifiot, Kasthuraiah Maddali, Alena Naumova, Xuemin Zhang, Christophe Marchand, and Yves Pommier*

Laboratory of Molecular Pharmacology, Center for Cancer Research, National Cancer Institute, National Institutes of Health, 37 Convent Drive, Bethesda, Maryland 20892

Received January 27, 2010; Revised Manuscript Received March 16, 2010

ABSTRACT: Resistance to raltegravir (RAL), the first HIV-1 integrase (IN) inhibitor approved by the FDA, involves three genetic pathways: IN mutations N155H, Q148H/R/K, and Y143H/R/C. Those mutations are generally associated with secondary point mutations. The resulting mutant viruses show a high degree of resistance against RAL but somehow are affected in their replication capacity. Clinical and virological data indicate the high relevance of the combination G140S + Q148H because of its limited impact on HIV replication and very high resistance to RAL. Here, we report how mutations at the amino acid residues 140, 148, and 155 affect IN enzymatic activity and RAL resistance. We show that single mutations at position 140 have limited impact on 3′-processing (3′-P) but severely inactivate strand transfer (ST). On the other hand, single mutations at position 148 have a more profound effect and inactivate both 3′-P and ST. By examining systematically all of the double mutants at the 140 and 148 positions, we demonstrate that only the combination G140S + Q148H is able to restore the catalytic properties of IN. This rescue only operates in *cis* when both the 140S and 148H mutations are in the same IN polypeptide flexible loop. Finally, we show that the G140S-Q148H double mutant exhibits the highest resistance to RAL. It also confers cross-resistance to elvitegravir but less to G-quadraduplex inhibitors such as zintevir. Our results demonstrate that IN mutations at positions 140 and 148 in the IN flexible loop can account for the phenotype of RAL-resistant viruses.

The first molecule approved for the treatment of HIV/AIDS[1] was zidovudine (AZT; GlaxoSmithKline), a chain terminator inhibiting the viral polymerase, reverse transcriptase (RT). AZT was approved by the FDA in March 1987. Over the past 25 years many RT inhibitors and protease (PR) inhibitors have been generated (a total of 22 drugs) (*1*) to overcome the selection of resistant viruses that appear quickly (6 months) in the AZT-treated patient (*2*). Highly active antiretroviral therapy (HAART) is generally composed of three to four drugs targeting at least two viral enzymes at a time. This regimen is very efficient. It reduces viral load and extends the lifetime of HIV-1-infected people. Unfortunately, even with multiple drugs and a very low replication rate, virus diversity (quasi-species) and the poor fidelity of RT still allow the emergence of resistance. In 2003, the first inhibitor of fusion was approved by the FDA followed in 2007 by the first integrase (IN) inhibitor, raltegravir (RAL). Today, the therapeutic armamentarium allows the targeting of four different steps of the HIV life cycle including the inhibition of all three viral enzymes (25 drugs in 31 formulations) (*3*).

IN is required *in vivo* for the integration of the reverse transcribed viral DNA within genomic DNA. This step of the viral cycle is part of four different processes requiring IN (*1*). Just after reverse transcription, IN becomes associated with the long terminal repeats (LTR) and processes the viral DNA ends along the motif CAGT. Cleavage of the 3′-extremities of the LTRs (terminal dinucleotide GT 3′ from the conserved CA dinucleotide) is catalyzed by at least a dimer of IN (*4*). This first activity, 3′-P processing (3′-P), is performed in the cytoplasm within a large nucleoprotein complex composed of viral and cellular cofactors (the preintegration complex, PIC). The PIC migrates along the microtubule network to the nucleus. Once in the nuclear compartment, the complex interacts with host DNA, and the integration of both viral DNA ends occurs 5 bp one from another on opposite strands of the same DNA duplex. This reaction, performed by at least a tetramer of IN (*4*), is referred to as strand transfer (ST). Inhibitors targeting this activity are called IN strand transfer inhibitors (INSTIs) (*1*, *5*). The last process involved in the completion of integration is the repair of the junctions between viral and cellular DNA. Those reactions are probably done by cellular enzymes and complete the integration of the viral DNA with a 5 bp duplication on each side. Both the 3′-P and ST reactions can be reproduced in biochemical assays using recombinant IN and short oligonucleotides derived from the LTR (*6*, *7*).

IN is a 32 kDa protein issued from the action of PR on the gag-pol precursor. IN can also be produced as recombinant and catalytically active enzyme (*6*−*8*). It is composed of three

[†]These studies were supported (in part) by the Intramural Research Program of the NIH, National Cancer Institute (NCI), Center for Cancer Research (CCR).

*To whom correspondence should be addressed at the Laboratory of Molecular Pharmacology, CCR, NCI, NIH, Building 37, Room 5068, Bethesda, MD 20892-4255. E-mail: pommier@nih.gov. Phone: 301-496-5944. Fax: 301-402-0752.

[1]Abbreviations: 3′-P, 3′-processing; AIDS, acquired immune deficiency syndrome; AZT, azidothymidine; EVG, elvitegravir; HAART, highly active antiretroviral therapy; HIV, human immunodeficiency virus; IC_{50}, inhibitory concentration 50%; IN, integrase; INSTI, integrase strand transfer inhibitor; LTR, long terminal repeat; Mo-MLV, Moloney murine leukemia virus; PIC, preintegration complex; PR, protease; RAL, raltegravir; RT, reverse transcriptase; ST, strand transfer; WT, wild type.

Published on Web 03/24/2010

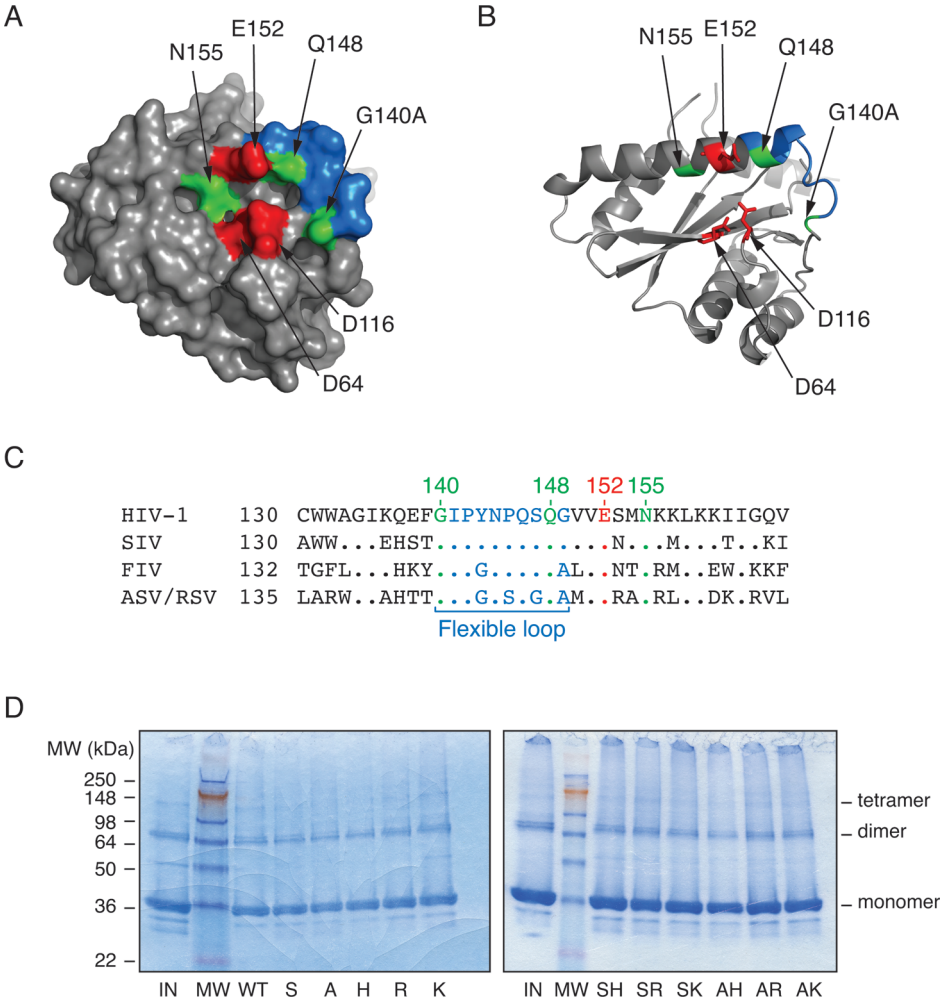

FIGURE 1: 3-D structure of HIV-1 IN and mutations investigated in the present study. (A, B) Crystal structure of HIV-1 IN. Amino acids implicated in RAL resistance (N155, G140, and Q148) are highlighted in green. Catalytic triads D64, D116, and E152 are represented in red, and the flexible loop residues (140−149) are colored in blue. This structure corresponds to the catalytic core of IN (50−212) with three point mutations (G140A, G149A, and F185K (PDB file 1bl3) (*17*). Surface (panel A) and cartoon (panel B) representations were obtained using MacPyMOLX11 hybrid. (C) Alignment of the sequence bordering and including the flexible loop of different IN (human immunodeficiency virus type 1, HIV-1; simian immunodeficiency virus, SIV; feline immunodeficiency virus, SIV; avian sarcoma virus, ASV; rous sarcoma virus, RSV). Amino acids identical to the HIV-1 IN sequence have been replaced by a period in other IN sequences. Numbering corresponds to HIV-1 IN. (D) SDS−PAGE of recombinant proteins mutated in their flexible loop and used in this study (10 μg/lane). IN corresponds to WT protein; MW, molecular weight markers (SeeBlue Plus 2 pretained standard; Invitrogen). Abbreviations for the mutant recombinant proteins: S, 140S; A, 140A; H, 148H; R, 148R; K, 148K; SH, 140S-148H; SR, 140S-148R; SK, 140S-148K; AH, 140A-148H; AR, 140A-148R; AK, 140A-148K.

domains (*9*, *10*). The N-terminus (amino acids 1−50) contains a zinc-binding motif $H_{12}H_{16}C_{40}C_{43}$ involved in the oligomerization of IN (*11*). The core domain (amino acids 50−212) contains the catalytic triad $D_{64}D_{116}E_{152}$ consisting in two aspartates and one glutamate residue. This DDE motif is well conserved across the retroviral integrase superfamily, part of the nuclease−transposase superfamilly (including, RNase H, Ruv C, transposases, and other retroviral integrases) (*12*). IN activities require the coordination of two divalent metal cofactors with the catalytic DDE triad and most likely together with the viral and host DNA. Although both Mn^{2+} and Mg^{2+} are effective *in vitro*, it is generally accepted that Mg^{2+} is the physiological metal (*10*). In the crystal structures, the DDE catalytic site is adjacent to a flexible loop, composed by residues 140−149 (see Figure 1A−C) (*13*), and which is also critical for catalysis. In particular, residue Q148 is implicated in the binding of the viral DNA and is critical for IN activities (*14*−*16*). The C-terminus (amino acids 212−288) contains a SH3-like domain and is involved in DNA binding. All three domains of IN form homodimers and are implicated in both the viral (donor) and the cellular (target) DNA binding.

To date, no 3-D structure of the full-length wild-type (WT) enzyme is available. Nevertheless, some structural data from truncated/mutant enzyme provide some insight of the global shape of the protein (*13*, *17*). Unfortunately, the flexible loop (amino acids 140−149) could not be totally resolved, and there is also no 3-D structure of IN−DNA complexes. This dramatically impairs the rational design of inhibitors.

The first IN inhibitor approved by the FDA, raltegravir (RAL, MK-0518; Merck), was originally introduced in regimen of heavily treated patients and is now also used in first line therapy (*18*−*22*). Specific mutations within the IN gene have already been identified in RAL-resistant patients (*23*−*25*). Three genetic resistance pathways with the primary substitutions Y143R/C, Q148H/R/K, and N155H have emerged in association with secondary mutations at positions E92Q/T97A/G163R, G140S/A, and E92Q/G, respectively (*23*, *26*, *27*). Such mutant viruses show a high degree of resistance against RAL but somehow are affected in their replication capacity depending on the mutation (*23*, *28*−*30*). Elvitegravir (EVG, GS-9137, JTK-303; Gilead) is the next most advanced currently in trials

(phase III) (*3*, *31*). Compared to RAL, EVG is more potent both *in vitro* and *ex vivo* (*15*, *32*) but also exhibits a higher toxicity in noninfected cells (*33*). Another limitation of EVG comes from its inactivation by cellular enzymes (*34*, *35*), which can be improved by coadministration with ritonavir (*35*). Regarding resistance mutations, we recently showed cross-resistance between EVG and RAL for a panel of point mutant IN (*15*). However, our prior study did not include the mutations that have now emerged from the clinical use of RAL.

In vivo data already suggest that the mutation combination G140S-Q148H is the most relevant one with a very slight impact on virus replication and the highest increase in resistance factor (*23*, *27*, *36*). In this particular case, it has been shown that mutation G140S rescued the defective phenotype of mutation Q148H (*28*). In the present study, we investigated the impact of mutations at positions 140 and 148 on the activity of resulting IN and on resistance properties.

MATERIALS AND METHODS

Oligonucleotide Synthesis and Drugs. Oligonucleotides were purchased from Integrated DNA Technologies, Inc. (Coralville, IA). Oligonucleotides 21t (GTGTGGAAAATCTCTAGCAGT), 19t (GTGTGGAAAATCTCTAGCA), and 21b (ACTGCTAGAGATTTTCCACAC) were used to generate the *in vitro* substrates for IN assays. Single-stranded oligonucleotides 21t and 19t were labeled at the 5′-end using T4 polynucleotide kinase (New England Biolabs, Ipswich, MA) with [γ-^{32}P]-ATP (Perkin-Elmer Life and Analytical Sciences, Boston, MA) according to the manufacturers' instructions. Unincorporated isotopes were removed using the Mini Quick spin oligo columns (Roche). The DNA duplexes 21t/21b (blunt-ended substrate, 21/21) and 19t/21b (precleaved substrate, 19/21) were annealed by addition of an equal concentration of the complementary strand, heating to 95 °C, and slow cooling to room temperature.

Primers used for site-directed mutagenesis, G140S (TCAAGCAGGAATTTAGCATTCCCTACAATCC), G140A (TCAAGCAGGAATTTGCCATTCCCTACAATCC), Q148H (CCCTACAATCCCCAAAGTCACGGGGTAATAG), Q148R (CCCTACAATCCCCAAAGTCGCGGGGTAATAG), Q148K (CCCTACAATCCCCAAAGTAAAGGGGTAATAG), and N155H (CTTTAATTCTTTATGCATAGATTCTATTACCCCCTG), correspond to the coding strand. The reverse complementary strand for each primer was also used. Mutated codons are underlined.

Raltegravir (RAL, MK-0518) was purified and elvitegravir (EVG, JTK-303) synthesized as described previously (*15*). Oligonucleotides 93del (GGGGTGGGAGGAGGGT) and T30923 [$(GGGT)_4$] were ordered lyophilized from IDT and resuspended upon arrival with potassium buffer (50 mM Tris-HCl, pH 7.5, and 10 mM KCl). G-quartets were formed by heating the samples at 98 °C for 5 min and slow cooling to room temperature before storage at −20 °C.

Mutagenesis. IN mutants were generated using the Stratagene QuikChange site-directed mutagenesis kit (La Jolla, CA), according to the manufacturer's instructions. The presence of the desired mutations and the integrity of the IN sequence were verified by DNA sequencing.

Integrase Purification. Recombinant wild-type (WT) or mutant IN polypeptides were purified from *Escherichia coli* as described (*37*). Briefly, the IN gene was cloned into pET15b plasmid (Novagen, Madison, WI) allowing the expression of the N-terminal 6-His-tagged protein under IPTG induction (isopropyl β-D-1-thiogalactopyranoside; Sigma). After mutagenesis, WT and mutant enzymes were expressed in *E. coli* and purified using a Ni column (fast-flow chelating Sepharose; GE Healthcare). To allow the purification of multiple enzymes in parallel, we used the Vac-Man lab vacuum manifold (Promega, Madison, WI) with Poly-Prep chromatography columns (Bio-Rad, Hercules, CA). All of the enzymes used in this study retained the N-terminal His tag.

Integrase Reactions. IN reactions were carried out by mixing 20 nM DNA with 400 nM IN (unless otherwise indicated) in a buffer containing 50 mM MOPS, pH 7.2, 7.5 mM $MgCl_2$, 14 mM 2-mercaptoethanol, and drugs or 10% DMSO (dimethyl sulfoxide, the drug solvant). Reactions were performed at 37 °C for 120 min unless otherwise indicated and quenched by addition of an equal volume of loading buffer [formamide containing 1% SDS (sodium dodecyl sulfate), 0.25% bromophenol blue, and xylene cyanol]. Reaction products were separated in 16% polyacrylamide denaturing sequencing gels. Dried gels were visualized using a Typhoon 8600 (GE Healthcare, Piscataway, NJ). Densitometric analysis was performed using ImageQuant 5.1 software from GE Healthcare.

RESULTS

Mutagenesis and Purification of Mutant IN Polypeptides. To elucidate the role of the flexible loop for IN activity and resistance to INSTIs, we generated a panel of mutations at amino acid positions 140 and 148, commonly mutated in RAL-resistant patients (Figure 1). The glycine residue at position 140 was mutated to serine (G140S) or alanine (G140A), and the glutamine residue at position 148 was mutated to histidine (Q148H), arginine (Q148R), or lysine (Q148K). All combinations of double mutations at these same positions were also engineered (SH, SR, SK, AH, AR, and AK). We also mutated the asparagine at position 155 to histidine (N155H) because it has been reported in RAL-resistant patients (*38*, *39*). After sequencing, we confirmed the introduction of the clinically reported mutations in the IN encoding plasmid pET15b. Recombinant enzymes were expressed and purified (Figure 1D).

Biochemical Activities of Mutant INs. First, we assessed the catalytic properties of the IN mutants using time−course experiments in gel-based assays. Using the full-length substrate corresponding to the viral U5 DNA end (21/21 duplex), we determined simultaneously both the 3′-P and coupled ST activities of the recombinant proteins (Figure 2). The two mutations at position 140 (G to S and G to A) preferentially affected ST activity while having limited impact on 3′-P (Figure 2A). For the mutants at position 148, both ST and 3′-P were severely abolished. When we looked at the double mutants, only the combination G140S-Q148H (SH) appeared almost fully active for both 3′-P and ST (Figure 2B). The combination SK was the only other one to show some remaining 3′-P activity with 45% of the WT level (Figure 2E).

Because of the defective 3′-P activity of some of the mutants, we directly examined their ST activity using the same gel-based assay but with a precleaved substrate (19/21 duplex) corresponding to the 3′-P product (*1*, *6*, *40*, *41*). Under these conditions, only the SH mutant was able to catalyze ST close to WT levels (Figure 2C,D). All of the other single and double mutations had a ST activity below 30% of WT activity. A summary of the biochemical activities of all of the mutants at positions 140 and 148 is displayed in Figure 2E.

Complementation Experiments. We next tested whether the rescue of activity observed in the double mutant G140S-Q148H required the mutations G140S and Q148H to be in the same molecule (*cis*) or in two distinct molecules (*trans*) forming the active dimers or tetramers (*4*). The activity of the double mutant (SH) was compared to a mixture of the single mutants (S + H, Figure 3). Because the results presented in Figure 2 were done with 400 nM enzyme, we first tested the mix of the 140S mutant at 200 nM plus the 148H mutant at 200 nM. The resulting ST activity was not raised above that of each single mutant alone (Figure 3B). When doubling the amount of enzyme (400 nM each single mutant leading to 800 nM total enzyme in the reaction mix), the ST activity was still not increased to the level of the SH double mutant (Figure 3A,C). These experiments demonstrate that the G140S and Q148H mutations need to be in the same IN molecule to complement each other.

Effect of the 140−148 Flexible Loop Mutations on RAL Resistance. Inhibition of the ST activity of the WT and the S, H, and SH mutant enzymes was examined in the presence of a range of RAL concentrations (Figure 4A). Quantification of ST products shows clear RAL concentration−response for the four enzymes in the range of concentrations used (Figure 4B). The IC_{50} of RAL for WT was around 70 nM. The Q148H mutant showed resistance to RAL with a 2− 3-fold increase in the IC_{50}

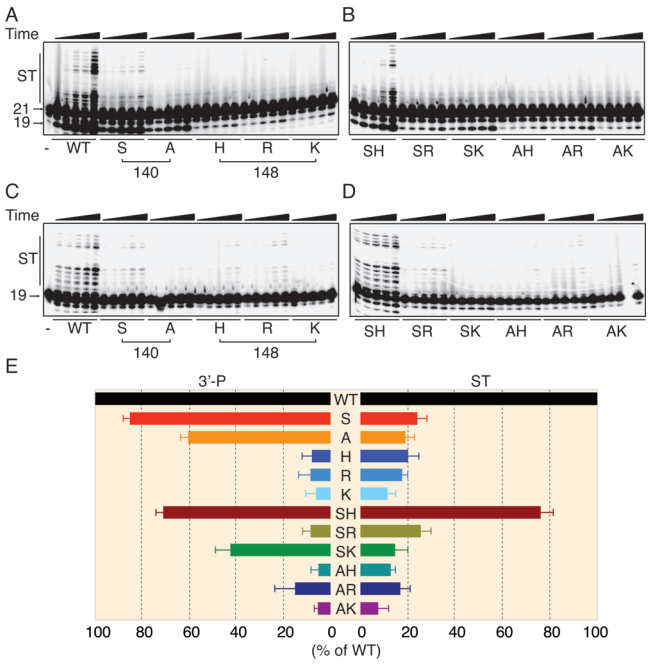

FIGURE 2: Biochemical activities of mutant IN enzymes. (A−D) Time−course experiments of 3′-processing (3′-P; panels A and B) and strand transfer (ST; panels C and D) were performed using a gel-based assay. Reactions were performed with the 21/21 full-length (panels A and B) or 19/21 precleaved substrates (panels C and D). Activities of WT and single mutant enzymes, including G140S/A, Q148H/R/K, are represented in panels A and C. Activities of the double mutants (six combinations G140S/A-Q148H/R/K) are represented in panels B and D. Reactions were performed at 37 °C for 15, 30, 45, 60, and 120 min and stopped with the addition of an equal volume of loading buffer. (E) Summary of the 3′-P (using the 21/21 substrate) and ST (using the 19/21 substrate) activities for the 12 enzymes measured after 120 min incubation at 37 °C. Means and standard deviations (SD) are from three to nine independent determinations. Values are reported on each side of the graphic (means ± SD).

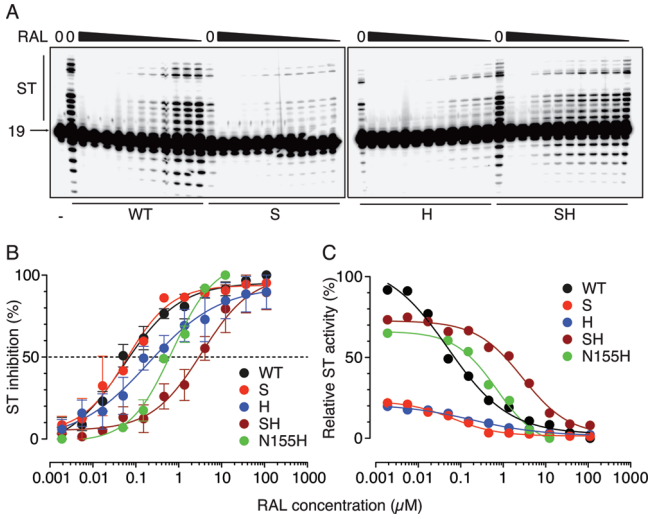

FIGURE 4: Activity of RAL on the ST activity of the IN mutants. (A) Representative gel showing the ST activity of WT, G140S (S), Q148H (H), and G140S-Q148H (SH) IN in the presence of RAL (from 111 μM to 1.9 nM in a 3-fold decrement). Reactions were performed using the precleaved 19/21 substrate at 37 °C for 120 min before loading on 16% PAGE. (B) Inhibition of ST is quantified including data for the IN mutant N155H. Mean and standard deviations derived from at least three independent determinations. (C) ST activity of WT and mutant IN in the presence of increasing concentrations of RAL. Data were obtained by transformation of panel B data.

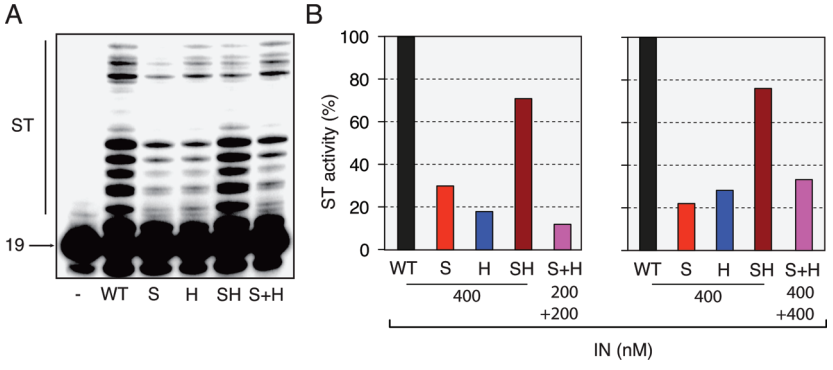

FIGURE 3: *cis*-complementation for the G140S-Q148H double mutant. (A) ST activity of WT, G140S (S), Q148H (H), and G140S-Q148H (SH) at 400 nM and a mixture of 400 nM G140S plus 400 nM Q148H (800 nM total enzyme, S + H). Reactions were performed at 37 °C for 120 min using the 19/21 precleaved substrate. (B) Quantification of the representative experiment shown in panel A (right histogram). The same experiment was performed using 200 nM IN mutant G140S with 200 nM Q148H for a total amount of enzyme of 400 nM, and quantification of a representative experiment is shown (left histogram).

(≈180 nM) while the G140S mutant appears as susceptible to RAL as the WT enzyme. In contrast, the SH double mutant showed an IC_{50} shift to 3 μM and a high degree of resistance to RAL (≈43-fold).

Regarding the other mutants (A, R, K, SR, SK, AH, AR, and AK), the very low level of activity of several combinations precluded accurate densitometric analysis. However, we visually scored the resistance profile to RAL, and those scores are summarized in Table 1. We also performed parallel experiments using the clinically relevant mutation N155H and found that the resistance of this enzyme was intermediate between the SH and WT enzymes with an IC_{50} of 600 nM (Figure 4B).

To emphasize the selective advantage of each mutation in the presence of RAL, we plotted the ST activity of the mutants in the presence of RAL compared to WT (Figure 4C). The ST activity of the SH double mutant remained above 50% in the presence of 1 μM of RAL while, under these conditions, the ST activity of the WT enzyme was below 20%. On the other hand, the single mutants G140S and Q148H are not able to produce more ST than WT at any of the RAL concentrations examined, and the N155H mutant shows only a slightly increased ST activity between 30 nM and 2.5 μM of RAL as compared to WT. These results demonstrate the selective advantage of the SH double mutant in the presence of RAL.

Table 1: Enzymatic Activity and Resistance of IN Mutants

enzyme	3′-P[a]	ST[a]	resistance[b]
WT	++++	++++	−
S	++++	++	−
A	+++	+	+
H	−	+	+
R	−	+	+
K	−	+	+
SH	++++	++++	+++
SR	−	++	+++
SK	+++	+	++
AH	−	+	++
AR	+	+	+++
AK	−	−	+

[a]3′-P (using the full-length substrate) and ST (using the precleaved substrate) activities are scored as percent WT activity: (−) <10%; (+) 10−20%; (++) 20−40%; (+++) 40−70%; (++++) 70−100%. [b]RAL IC_{50} increase is scored compared to WT: (−) 1-fold; (+) 2−3-fold; (++) 10−25-fold; (+++) up to 50-fold.

Effect of 140S-148H Mutations on 3′-P Inhibition by RAL. Although RAL is a potent ST inhibitor, it is also active on 3′-P activity at high concentrations (reported selectivity index around 150) (*15*). Thus, we investigated the effect of RAL on the 3′-P activity of the SH double mutant. Using the full-length substrate, we observed an inhibition of the 3′-P and ST activity of WT protein in the presence of RAL (Figure 5A). The IC_{50} for 3′-P was around 10.5 μM, consistent with a selectivity index of 150 for ST (Figure 5B). Figure 5 also shows that inhibition of 3′-P by RAL for the SH double mutant was observed at higher concentrations than for the WT enzyme (Figure 5A). The IC_{50} of RAL for the 3′-P activity of the mutant was over 650 μM corresponding to more than 62-fold increase compared to WT (Figure 5B). Similarly to the relative ST activity, we determined the relative 3′-P activity of the SH mutant compared to WT without RAL (Figure 5C). In this case, as for ST, inhibition of the SH double mutant required a RAL concentration 30 times higher than the concentration required to induce a comparable inhibition of the WT protein.

Cross-Resistance of the 140S-148H Double Mutant to EVG. We next investigated the effect of EVG on the ST activity of the WT and SH mutant enzymes (Figure 6A). ST activity of WT protein was inhibited with the lowest concentrations of EVG used (in the low nanomolar range). ST products resulting from the SH mutant activity were still observed in the same range of concentrations, and the inhibition was observed only for higher concentration (low micromolar inhibition). Quantifications show

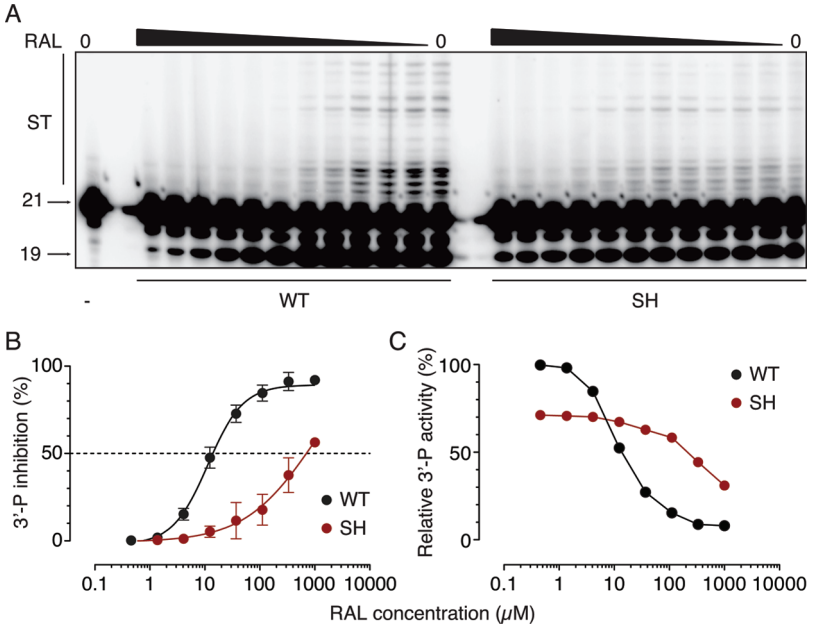

FIGURE 5: Resistance of the 3′-P activity of the IN G140S-Q148H mutant to RAL. (A) Representative gel showing the 3′-P activity of WT and G140S-Q148H (SH) IN in the presence of RAL (from 333 μM to 5.6 nM in a 3-fold decrement). Reactions were performed using the blunt-ended 21/21 substrate at 37 °C for 120 min before loading on a 16% PAGE. (B) Inhibition of 3′-P was quantified for at least three independent experiments (means and standard deviations). (C) 3′-P activity of WT and mutant IN in the presence of increasing concentrations of RAL compared to WT. Data were obtained by transformation of panel B data.

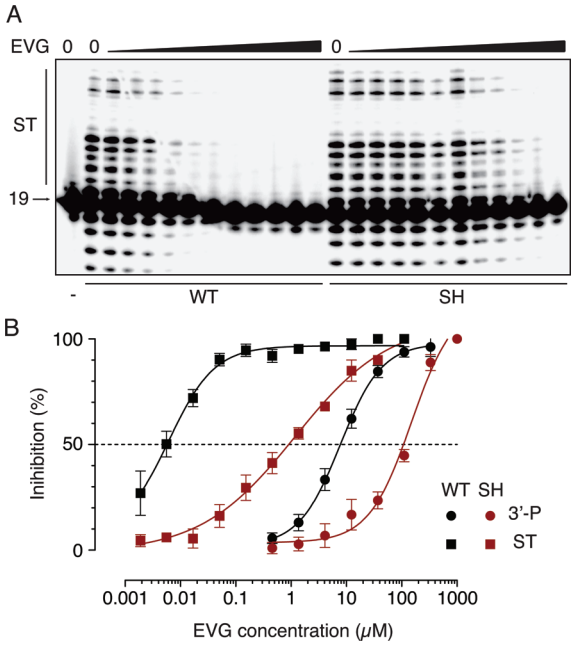

FIGURE 6: Resistance of the G140S-Q148H mutant to EVG. (A) Representative gel showing the ST activity of WT and G140S-Q148H (SH) IN in the presence of EVG (from 1.9 nM to 111 μM in a 3-fold increment). Reactions were performed using the precleaved 19/21 substrate at 37 °C for 120 min before loading on 16% PAGE. (B) Quantification of 3′-P inhibition (using the blunt-ended 21/21 substrate; PAGE not shown) and ST inhibition. Means and standard deviations were derived from at least three independent determinations.

a shift in the IC_{50} from 6 nM for the WT protein to 1 μM for the SH double mutant (Figure 6B). Regarding 3′-P activity, WT enzyme was inhibited by EVG with an IC_{50} of 8 μM, and the SH double mutant showed a 12−13-fold resistance factor with an IC_{50} of 100 μM (Figure 6B).

Overcoming the Resistance of the SH Mutant with Other Chemotypes. G-quartet-forming oligonucleotides are well established IN inhibitors (*42*−*46*). We studied the 3′-P and ST inhibition of both WT and double mutant SH IN by the aptamer 93del (GGGGTGGGAGGAGGGT) and by a zintevir analogue, T30923 (GGGTGGGTGGGTGGGT). As already reported (*43*), the WT enzyme was inhibited by 93del with an IC_{50} for ST of 100 nM (data not shown). More noticeably, the SH double mutant was inhibited in the same range of concentration as WT. We next evaluated the 3′-P inhibition of WT and SH double mutant enzymes by 93del using the full-length DNA substrate (data not shown). The SH double mutation induced a small increase in IC_{50} from 0.2 μM for WT to 1.5 μM for the SH double mutant (8-fold). We also performed similar experiments with an analogue of zintevir, T30923 (GGGTGGGTGGGTGGGT) (*44*). T30923 inhibited the ST activity of WT enzyme with a lower IC_{50} than 93del (10 nM; data not shown). With a 3-fold increase in IC_{50}, T30923 showed minimal impact on the ST inhibition of the SH double mutant (data not shown). When we looked at the 3′-P inhibition (with the full-length substrate; data not shown), the inhibition profile with T30923 was comparable to the profile with 93del. The SH double mutation induced a small increase in IC_{50} for 3′-P inhibition by T30923 from 200 nM for WT to 1 μM for the SH double mutant (5-fold).

DISCUSSION

To date, no 3-D structure is available for the full-length active IN or for IN bound to DNA. Only isolated domains have been solved, twice in the presence of a ligand (*47*, *48*). In contrast to the catalytic triad DDE (see Figure 1), which is always defined with metal cofactor, the segment encompassing amino acid residues 140−149 is consistently not well resolved due to low diffraction. That segment is commonly referred to as the flexible loop (*9*, *10*). The flexibility of the 140−149 segment is probably due at least in part to the presence of two glycines (G140 and G149) at each end acting as hinges. Glycine is the amino acid with the smallest side chain, which intrinsically enables the highest degree of rotation of the polypeptide backbone. Mutating residues 140 and 149 to alanine allowed the complete resolution of the loop, suggesting that the loop with those mutated hinge residues is less flexible (*17*).

Here we show that single mutations at position 140, from glycine to serine or to alanine, impair ST activity without inactivating 3′-P (see Figure 2). To date, residue G140 has not been reported to directly interact with DNA. It is generally accepted that IN undergoes a conformational change between 3′-P and ST to accommodate the target (host chromosomal) DNA in the catalytic site of the enzyme while the processed 3′-end of the viral DNA becomes the nucleophile and the target of INSTI (*1*, *5*). The G140S/A mutants could allow an effective interaction with the viral DNA, which would lead to its preserved ability to catalyze 3′-P. This mutant is however not able to catalyze ST. Possibly, this might be due to conformational restriction. Indeed, a recent study on Moloney murine leukemia virus (Mo-MLV) IN proposed a direct correlation between flexibility of the loop and ST activity. Mutations that reduced flexibility specifically impaired ST but not 3′-P or disintegration (*49*). In the context of the virus, the mutation G140S is known to delay viral replication. This delay was attributed to a lack of integration (*50*, *51*). Our present study suggests this defect is primarily due to impaired ST.

Mutations at position 148 to histidine, arginine, or lysine totally inactivated the enzyme for both the 3′-P and ST reactions. In the normal (WT) IN, the glutamine residue at position 148 and the tyrosine 143 of the flexible loop have been shown to interact with the tip of the viral DNA LTR (*52*). More precisely, chemical cross-linking studies showed a direct interaction between the IN residue at position 148 and the 5′-C on the overhang of the viral DNA lower strand (*14*, *37*). Changing this glutamine residue to histidine, arginine, or lysine, which have larger and longer side chains, probably alters viral DNA binding, thereby inhibiting both 3′-P and ST. Similarly, mutating Q148 to alanine, asparagine, or cysteine was previously shown to block ST activity (*14*). *In vivo*, mutations at position 148 markedly decrease the replication capacity of mutant viruses (*3*, *23*). Our data suggest such defects are primarily due to inactivation of both the 3′-P and ST activities of IN.

Simultaneous mutations at both sites (140S and 148H) restored the catalytic activities of the resulting enzyme to almost WT levels and most notably to levels well above each of the single mutants (see Figures 2 and 3). Our data demonstrate this complementation operates in *cis*; i.e., both mutations have to be present within the same IN molecule (see Figure 3). Indeed, mixing two single mutants failed to rescue enzymatic activity. The rescue was only possible with the combination SH (see Figure 2). Any other combination tested (SR, SK, AH, AR, or AK) at best only partially affected IN activities (SK mutant, only improving 3′-P). The finding that the flexible loop mutants do not complement each other if they are on different IN molecules is consistent with prior study showing that active site mutants (on the DDE motif) do not complement each other in *trans* (*53*). These results

demonstrate the interdependency of residues 140 and 148 for IN catalytic activity. Structural studies are warranted to determine whether the SH double mutant IN will reveal the position of the flexible loop in an active configuration.

Appearance of mutations in patients seems to be dependent on the time of exposure to RAL. The N155 pathway is generally the first one to emerge. Our data show that this mutation confers approximately 10-fold resistance to RAL but also reduces IN's intrinsic enzymatic activity (see Figure 4). Viruses with the double mutation G140-Q148 appear as treatment is prolonged (*36*). Single point mutations in the IN nucleic acid coding sequence are sufficient to produce all of the clinically relevant mutants at positions 140 and 148 examined here. Mutation G140S was first reported for resistance to L-CA (*50*, *51*) and more recently has been found to also confer minimal resistance to RAL and some diketo acids (*28*, *54*). Here, we show no detectable resistance of the G140S mutant to RAL (see Figure 4) or EVG (data not shown). In contrast, we find all of the clinically relevant 148 mutants (Q148H/R/K) resistant to RAL (see Figure 4). However, all of those single mutants present replicative defects (*23*). Accordingly, we found that those IN mutants are catalytically impaired (see Figures 2 and 4). Moreover, Figure 4C shows that the enzymatic activity of all of the single mutants at position Q148 is less than that of the WT enzyme in the presence of RAL. This phenotype could explain the tendency of the 148 single mutants to be quickly replaced by the 140S-148H double mutants *in vivo*.

While all of the single mutants impaired IN's catalytic activity, here we show that the clinically relevant mutant G140S-Q148H, which reestablishes an active site able to carry out both 3′-P and ST, also is highly resistant to RAL or EVG. Thus, our experiments demonstrate that the SH double mutation does not restore a proper drug binding site for RAL or EVG. Notably, the SH double mutant IN was also resistant to 3′-P inhibition by RAL and EVG (see Figures 5 and 6). Thus, in spite of the fact that the 3′-P and ST sites may have different conformations, the SH double mutation alters both sites as revealed by RAL and EVG resistance for both 3′-P and ST. Considering that drug resistance affects not only ST but also 3′-P indicates that RAL and EVG can bind IN in the context of a complex with or without the viral DNA and that the drug binding site in those two conditions involves the flexible loop.

Finally, we show that other kinds of inhibitors such as guanosine quartet oligonucleotides could completely inhibit the SH-resistant mutant (data not shown). G-quadraduplexes have been shown to be nontoxic and able to cross the cell membrane, allowing a potential inhibition of intracellular targets (*45*, *46*). Unfortunately, resistant viruses to zintevir presented mutations in the gp120 coding gene, showing that IN was not the primary target of this inhibitor (*55*). These results show that the SH double mutant could be directly used to identify new inhibitors to overcome resistance to RAL and EVG. Altogether, our study provides a new insight on the role played by the IN flexible loop during the integration process and drug response. These results may guide future structural studies to better model the IN active site and allow the development of next generation IN inhibitors to overcome RAL resistance.

ACKNOWLEDGMENT

We wish to thank Dr. Craig Thomas, NIH Chemical Genomic Center (NCGC, Rockville, MD) for providing raltegravir and elvitegravir.

REFERENCES

1. Pommier, Y., Johnson, A. A., and Marchand, C. (2005) Integrase inhibitors to treat HIV/AIDS. *Nat. Rev. Drug Discovery 4*, 236–248.
2. Larder, B. A., Darby, G., and Richman, D. D. (1989) HIV with reduced sensitivity to zidovudine (AZT) isolated during prolonged therapy. *Science 243*, 1731–1734.
3. Marchand, C., Maddali, K., Metifiot, M., and Pommier, Y. (2009) HIV-1 IN inhibitors: 2010 update and perspectives. *Curr. Top. Med. Chem. 9*, 1016–1037.
4. Faure, A., Calmels, C., Desjobert, C., Castroviejo, M., Caumont-Sarcos, A., Tarrago-Litvak, L., Litvak, S., and Parissi, V. (2005) HIV-1 integrase crosslinked oligomers are active in vitro. *Nucleic Acids Res. 33*, 977–986.
5. Espeseth, A. S., Felock, P., Wolfe, A., Witmer, M., Grobler, J., Anthony, N., Egbertson, M., Melamed, J. Y., Young, S., Hamill, T., Cole, J. L., and Hazuda, D. J. (2000) HIV-1 integrase inhibitors that compete with the target DNA substrate define a unique strand transfer conformation for integrase. *Proc. Natl. Acad. Sci. U.S.A. 97*, 11244–11249.
6. Craigie, R., Mizuuchi, K., Bushman, F. D., and Engelman, A. (1991) A rapid in vitro assay for HIV DNA integration. *Nucleic Acids Res. 19*, 2729–2734.
7. Fesen, M. R., Kohn, K. W., Leteurtre, F., and Pommier, Y. (1993) Inhibitors of human immunodeficiency virus integrase. *Proc. Natl. Acad. Sci. U.S.A. 90*, 2399–2403.
8. Goodarzi, G., Im, G. J., Brackmann, K., and Grandgenett, D. (1995) Concerted integration of retrovirus-like DNA by human immunodeficiency virus type 1 integrase. *J. Virol. 69*, 6090–6097.
9. Chiu, T. K., and Davies, D. R. (2004) Structure and function of HIV-1 integrase. *Curr. Top. Med. Chem. 4*, 965–977.
10. Jaskolski, M., Alexandratos, J. N., Bujacz, G., and Wlodawer, A. (2009) Piecing together the structure of retroviral integrase, an important target in AIDS therapy. *FEBS J. 276*, 2926–2946.
11. Zheng, R., Jenkins, T. M., and Craigie, R. (1996) Zinc folds the N-terminal domain of HIV-1 integrase, promotes multimerization, and enhances catalytic activity. *Proc. Natl. Acad. Sci. U.S.A. 93*, 13659–13664.
12. Nowotny, M. (2009) Retroviral integrase superfamily: the structural perspective. *EMBO Rep. 10*, 144–151.
13. Maignan, S., Guilloteau, J. P., Zhou-Liu, Q., Clement-Mella, C., and Mikol, V. (1998) Crystal structures of the catalytic domain of HIV-1 integrase free and complexed with its metal cofactor: high level of similarity of the active site with other viral integrases. *J. Mol. Biol. 282*, 359–368.
14. Johnson, A. A., Santos, W., Pais, G. C., Marchand, C., Amin, R., Burke, T. R., Jr., Verdine, G., and Pommier, Y. (2006) Integration requires a specific interaction of the donor DNA terminal 5′-cytosine with glutamine 148 of the HIV-1 integrase flexible loop. *J. Biol. Chem. 281*, 461–467.
15. Marinello, J., Marchand, C., Mott, B. T., Bain, A., Thomas, C. J., and Pommier, Y. (2008) Comparison of raltegravir and elvitegravir on HIV-1 integrase catalytic reactions and on a series of drug-resistant integrase mutants. *Biochemistry 47*, 9345–9354.
16. Lu, R., Limon, A., Ghory, H. Z., and Engelman, A. (2005) Genetic analyses of DNA-binding mutants in the catalytic core domain of human immunodeficiency virus type 1 integrase. *J. Virol. 79*, 2493–2505.
17. Greenwald, J., Le, V., Butler, S. L., Bushman, F. D., and Choe, S. (1999) The mobility of an HIV-1 integrase active site loop is correlated with catalytic activity. *Biochemistry 38*, 8892–8898.
18. FDA notifications (2009) FDA approves raltegravir for HIV-1 treatment-naive patients. *AIDS Alert 24*, 106–107.
19. Cocohoba, J. (2009) The SWITCHMRK studies: substitution of lopinavir/ritonavir with raltegravir in HIV-positive individuals. *Expert Rev. Anti-Infect. Ther. 7*, 1159–1163.
20. Emery, S., and Winston, A. (2009) Raltegravir: a new choice in HIV and new chances for research. *Lancet 374*, 764–766.
21. Garrido, C., Soriano, V., and de Mendoza, C. (2010) New therapeutic strategies for raltegravir. *J. Antimicrob. Chemother. 65*, 218–223.
22. Lennox, J. L., DeJesus, E., Lazzarin, A., Pollard, R. B., Madruga, J. V., Berger, D. S., Zhao, J., Xu, X., Williams-Diaz, A., Rodgers, A. J., Barnard, R. J., Miller, M. D., DiNubile, M. J., Nguyen, B. Y., Leavitt, R., and Sklar, P. (2009) Safety and efficacy of raltegravir-based versus efavirenz-based combination therapy in treatment-naive patients with HIV-1 infection: a multicentre, double-blind randomised controlled trial. *Lancet 374*, 796–806.

23. Fransen, S., Gupta, S., Danovich, R., Hazuda, D., Miller, M., Witmer, M., Petropoulos, C. J., and Huang, W. (2009) Loss of raltegravir susceptibility by human immunodeficiency virus type 1 is conferred via multiple nonoverlapping genetic pathways. *J. Virol. 83*, 11440–11446.
24. Lataillade, M., Chiarella, J., and Kozal, M. J. (2007) Natural polymorphism of the HIV-1 integrase gene and mutations associated with integrase inhibitor resistance. *Antivir. Ther. 12*, 563–570.
25. Markowitz, M., Nguyen, B. Y., Gotuzzo, E., Mendo, F., Ratanasuwan, W., Kovacs, C., Prada, G., Morales-Ramirez, J. O., Crumpacker, C. S., Isaacs, R. D., Gilde, L. R., Wan, H., Miller, M. D., Wenning, L. A., and Teppler, H. (2007) Rapid and durable antiretroviral effect of the HIV-1 integrase inhibitor raltegravir as part of combination therapy in treatment-naive patients with HIV-1 infection: results of a 48-week controlled study. *J. Acquir. Immune Defic. Syndr. 46*, 125–133.
26. Baldanti, F., Paolucci, S., Gulminetti, R., Brandolini, M., Barbarini, G., and Maserati, R. (2010) Early emergence of raltegravir resistance mutations in patients receiving HAART salvage regimens. *J. Med. Virol. 82*, 116–122.
27. Quercia, R., Dam, E., Perez-Bercoff, D., and Clavel, F. (2009) Selective-advantage profile of human immunodeficiency virus type 1 integrase mutants explains in vivo evolution of raltegravir resistance genotypes. *J. Virol. 83*, 10245–10249.
28. Delelis, O., Malet, I., Na, L., Tchertanov, L., Calvez, V., Marcelin, A. G., Subra, F., Deprez, E., and Mouscadet, J. F. (2009) The G140S mutation in HIV integrases from raltegravir-resistant patients rescues catalytic defect due to the resistance Q148H mutation. *Nucleic Acids Res. 37*, 1193–1201.
29. Delelis, O., Thierry, S., Subra, F., Simon, F., Malet, I., Alloui, C., Sayon, S., Calvez, V., Deprez, E., Marcelin, A. G., Tchertanov, L., and Mouscadet, J. F. (2010) Impact of Y143 HIV-1 integrase mutations on resistance to raltegravir in vitro and in vivo. *Antimicrob. Agents Chemother. 54*, 491–501.
30. Malet, I., Delelis, O., Soulie, C., Wirden, M., Tchertanov, L., Mottaz, P., Peytavin, G., Katlama, C., Mouscadet, J. F., Calvez, V., and Marcelin, A. G. (2009) Quasispecies variant dynamics during emergence of resistance to raltegravir in HIV-1-infected patients. *J. Antimicrob. Chemother. 63*, 795–804.
31. Shimura, K., and Kodama, E. N. (2009) Elvitegravir: a new HIV integrase inhibitor. *Antivir. Chem. Chemother. 20*, 79–85.
32. Kobayashi, M., Nakahara, K., Seki, T., Miki, S., Kawauchi, S., Suyama, A., Wakasa-Morimoto, C., Kodama, M., Endoh, T., Oosugi, E., Matsushita, Y., Murai, H., Fujishita, T., Yoshinaga, T., Garvey, E., Foster, S., Underwood, M., Johns, B., Sato, A., and Fujiwara, T. (2008) Selection of diverse and clinically relevant integrase inhibitor-resistant human immunodeficiency virus type 1 mutants. *Antivir. Res. 80*, 213–222.
33. Sato, M., Motomura, T., Aramaki, H., Matsuda, T., Yamashita, M., Ito, Y., Kawakami, H., Matsuzaki, Y., Watanabe, W., Yamataka, K., Ikeda, S., Kodama, E., Matsuoka, M., and Shinkai, H. (2006) Novel HIV-1 integrase inhibitors derived from quinolone antibiotics. *J. Med. Chem. 49*, 1506–1508.
34. Pace, P., and Rowley, M. (2008) Integrase inhibitors for the treatment of HIV infection. *Curr. Opin. Drug Discovery Dev. 11*, 471–479.
35. Ramanathan, S., Shen, G., Hinkle, J., Enejosa, J., and Kearney, B. P. (2007) Pharmacokinetics of coadministered ritonavir-boosted elvitegravir and zidovudine, didanosine, stavudine, or abacavir. *J. Acquir. Immune Defic. Syndr. 46*, 160–166.
36. Fransen, S., Karmochkine, M., Huang, W., Weiss, L., Petropoulos, C. J., and Charpentier, C. (2009) Longitudinal analysis of raltegravir susceptibility and integrase replication capacity of human immunodeficiency virus type 1 during virologic failure. *Antimicrob. Agents Chemother. 53*, 4522–4524.
37. Johnson, A. A., Marchand, C., Patil, S. S., Costi, R., Di Santo, R., Burke, T. R., Jr., and Pommier, Y. (2007) Probing HIV-1 integrase inhibitor binding sites with position-specific integrase-DNA cross-linking assays. *Mol. Pharmacol. 71*, 893–901.
38. Charpentier, C., Karmochkine, M., Laureillard, D., Tisserand, P., Belec, L., Weiss, L., Si-Mohamed, A., and Piketty, C. (2008) Drug resistance profiles for the HIV integrase gene in patients failing raltegravir salvage therapy. *HIV Med. 9*, 765–770.
39. Cooper, D. A., Steigbigel, R. T., Gatell, J. M., Rockstroh, J. K., Katlama, C., Yeni, P., Lazzarin, A., Clotet, B., Kumar, P. N., Eron, J. E., Schechter, M., Markowitz, M., Loutfy, M. R., Lennox, J. L., Zhao, J., Chen, J., Ryan, D. M., Rhodes, R. R., Killar, J. A., Gilde, L. R., Strohmaier, K. M., Meibohm, A. R., Miller, M. D., Hazuda, D. J., Nessly, M. L., DiNubile, M. J., Isaacs, R. D., Teppler, H., and Nguyen, B. Y. (2008) Subgroup and resistance analyses of raltegravir for resistant HIV-1 infection. *N. Engl. J. Med. 359*, 355–365.
40. Bushman, F. D., and Craigie, R. (1991) Activities of human immunodeficiency virus (HIV) integration protein in vitro: specific cleavage and integration of HIV DNA. *Proc. Natl. Acad. Sci. U.S.A. 88*, 1339–1343.
41. Marchand, C., Neamati, N., and Pommier, Y. (2001) In vitro human immunodeficiency virus type 1 integrase assays. *Methods Enzymol. 340*, 624–633.
42. Cherepanov, P., Este, J. A., Rando, R. F., Ojwang, J. O., Reekmans, G., Steinfeld, R., David, G., De Clercq, E., and Debyser, Z. (1997) Mode of interaction of G-quartets with the integrase of human immunodeficiency virus type 1. *Mol. Pharmacol. 52*, 771–780.
43. de Soultrait, V. R., Lozach, P. Y., Altmeyer, R., Tarrago-Litvak, L., Litvak, S., and Andreola, M. L. (2002) DNA aptamers derived from HIV-1 RNase H inhibitors are strong anti-integrase agents. *J. Mol. Biol. 324*, 195–203.
44. Jing, N., Marchand, C., Liu, J., Mitra, R., Hogan, M. E., and Pommier, Y. (2000) Mechanism of inhibition of HIV-1 integrase by G-tetrad-forming oligonucleotides in vitro. *J. Biol. Chem. 275*, 21460–21467.
45. Mazumder, A., Neamati, N., Ojwang, J. O., Sunder, S., Rando, R. F., and Pommier, Y. (1996) Inhibition of the human immunodeficiency virus type 1 integrase by guanosine quartet structures. *Biochemistry 35*, 13762–13771.
46. Metifiot, M., Faure, A., Guyonnet-Duperat, V., Bellecave, P., Litvak, S., Ventura, M., and Andreola, M. L. (2007) Cellular uptake of ODNs in HIV-1 human-infected cells: a role for viral particles in DNA delivery? *Oligonucleotides 17*, 151–165.
47. Goldgur, Y., Craigie, R., Cohen, G. H., Fujiwara, T., Yoshinaga, T., Fujishita, T., Sugimoto, H., Endo, T., Murai, H., and Davies, D. R. (1999) Structure of the HIV-1 integrase catalytic domain complexed with an inhibitor: a platform for antiviral drug design. *Proc. Natl. Acad. Sci. U.S.A. 96*, 13040–13043.
48. Lubkowski, J., Yang, F., Alexandratos, J., Wlodawer, A., Zhao, H., Burke, T. R., Jr., Neamati, N., Pommier, Y., Merkel, G., and Skalka, A. M. (1998) Structure of the catalytic domain of avian sarcoma virus integrase with a bound HIV-1 integrase-targeted inhibitor. *Proc. Natl. Acad. Sci. U.S.A. 95*, 4831–4836.
49. Acevedo, M. L., Arbildua, J. J., Monasterio, O., Toledo, H., and Leon, O. (2009) Role of the 207−218 peptide region of Moloney murine leukemia virus integrase in enzyme catalysis, Arch. Biochem. Biophys. (in press).
50. King, P. J., Lee, D. J., Reinke, R. A., Victoria, J. G., Beale, K., and Robinson, W. E., Jr. (2003) Human immunodeficiency virus type-1 integrase containing a glycine to serine mutation at position 140 is attenuated for catalysis and resistant to integrase inhibitors. *Virology 306*, 147–161.
51. King, P. J., and Robinson, W. E., Jr. (1998) Resistance to the anti-human immunodeficiency virus type 1 compound L-chicoric acid results from a single mutation at amino acid 140 of integrase. *J Virol 72*, 8420–8424.
52. Esposito, D., and Craigie, R. (1998) Sequence specificity of viral end DNA binding by HIV-1 integrase reveals critical regions for protein-DNA interaction. *EMBO J. 17*, 5832–5843.
53. van Gent, D. C., Vink, C., Groeneger, A. A., and Plasterk, R. H. (1993) Complementation between HIV integrase proteins mutated in different domains. *EMBO J. 12*, 3261–3267.
54. Nakahara, K., Wakasa-Morimoto, C., Kobayashi, M., Miki, S., Noshi, T., Seki, T., Kanamori-Koyama, M., Kawauchi, S., Suyama, A., Fujishita, T., Yoshinaga, T., Garvey, E. P., Johns, B. A., Foster, S. A., Underwood, M. R., Sato, A., and Fujiwara, T. (2009) Secondary mutations in viruses resistant to HIV-1 integrase inhibitors that restore viral infectivity and replication kinetics. *Antivir. Res. 81*, 141–146.
55. Este, J. A., Cabrera, C., Schols, D., Cherepanov, P., Gutierrez, A., Witvrouw, M., Pannecouque, C., Debyser, Z., Rando, R. F., Clotet, B., Desmyter, J., and De Clercq, E. (1998) Human immunodeficiency virus glycoprotein gp120 as the primary target for the antiviral action of AR177 (Zintevir). *Mol. Pharmacol. 53*, 340–345.